Available online at www.sciencedirect.com
SCIENCE DIRECT®
Surface and Coatings Technology 171 (2003) 226–230
SURFACE & COATINGS TECHNOLOGY
www.elsevier.com/locate/surfcoat

Paradoxical sheath width variation in transversely magnetized capacitive coupled plasma

S.J. You*, K.H. Bai[1], J.H. In, H.Y. Chang, C.K. Choi[2]

Department of Physics, Korea Advanced Institute of Science and Technology, Daejeon 305 701, South Korea

Abstract

We investigated r.f. sheath width variation in transversely magnetized capacitive coupled plasma. While increasing the magnetic field, a paradoxical sheath width variation was observed. Although the electron density decreases with increasing magnetic field, the r.f. sheath width ($S_0 \propto 1/\sqrt{n_e}$) decreases with increasing magnetic field. This paradoxical result originates from the overlooking of the axial electron density profile variation by the magnetic field.

Keywords: R.f. sheath; Magnetic field; Capacitive coupled plasma

1. Introduction

Radio frequency capacitive discharge is wisely used in material processing such as thin film deposition, etching and sputtering [1–3]. Increasing the plasma processing in semi-conductor processing, a plasma parameter measurement has become a necessary work to improve its processing characteristics through understanding the physics in plasma processing. In the capacitive plasma discharge, there are many plasma parameters, such as electron density, electron temperature, r.f. sheath and plasma potential. Among these, the r.f. sheath is one of the most important plasma parameters in processing, because many of the physical processes in r.f. the sheath directly influence the surface reactions during the processing. The r.f. sheath is important not only in the plasma processing but also in r.f. plasma physics as a fundamental interest, such as low pressure collisionless heating [5,11,12]. Therefore, an understanding of the r.f. sheath characteristics is essential to understanding of the capacitive discharge.

There are many analytical studies about the r.f. sheath in the capacitive discharge [4–10] and the models proposed in these studies are well consistent with one another [13]. All previous models agree that the r.f. sheath width increases against decreasing current density (J_i) and increasing sheath voltage. Because the electron density is proportional to J_i, the sheath width decreases with the increasing electron density ($S_0 \propto 1/\sqrt{n_e}$). Moreover, it has been found that this relation holds even in the transversely magnetized capacitive discharge [14,15]. Therefore, it is well known that at a constant sheath voltage the r.f. sheath width decreases with increasing electron density.

In this paper, however, we present a paradoxical sheath width variation in the transversely magnetized capacitive discharge. Although the electron density decreases with the magnetic field, the r.f. sheath width decreases with the magnetic field. This result violates the relation ($S_0 \propto 1/\sqrt{n_e}$) presented in many previous report [4–6,14,15]. This paradoxical result originates from the overlooking of the axial electron density profile variation by the magnetic field. Therefore, this paradox could be solved successfully by considering the axial electron density profile of the transversely magnetized capacitive discharge.

2. Experimental details

Fig. 1 shows a schematic diagram of a transversely magnetized capacitive discharge system. The reactor is composed of two parallel electrodes which have different dimension, separated by 40 mm and asymmetrically driven at 13.56 MHz, argon. The lower one is the

*Corresponding author. Tel.: +82-42-869-2566; fax: +82-42-869-5526.
E-mail address: spinup@cais.kaist.ac.kr (S.J. You).
[1] Samsung Electronics.
[2] Department of Physics, Cheju National University, Cheju 390-756, South Korea.

0257-8972/03/$ - see front matter © 2003 Elsevier Science B.V. All rights reserved.
doi:10.1016/S0257-8972(03)00276-7

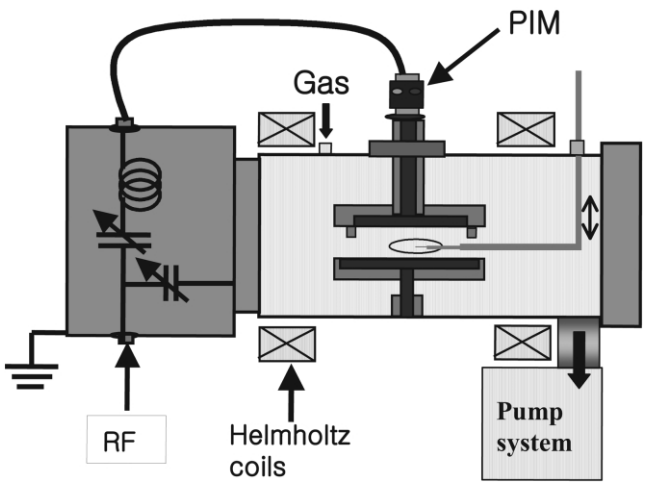

Fig. 1. Schematic diagram of a transversely magnetized CCP.

grounded electrode 200 mm in diameter and the upper one is the powered electrode 140 mm in diameter. The two electrodes are separated by 40 mm and positioned at the center of the discharge chamber. To keep the discharge between the two electrodes, a confinement-ring having a diameter equal to that of the powered electrode and a height of 10 mm is introduced beneath the powered electrode, and each electrode is wrapped by a ceramic cylinder slightly larger than the lower electrode and 50 mm in height.

External Helmholtz coils with inner diameters of 370 mm and widths of 70 mm are installed to make a DC magnetic field in the direction parallel to the electrode surface. A DC magnetic field has a uniformity within 5% up to 30 G. R.f. power (ENI, A1000) is delivered to the powered electrode through a standard L-type matching network and a coaxial cable.

To obtain the r.f. sheath width, we used the I–V measurement method ($S_0 \sim \varepsilon_0 A/C_{sh}$) [13,16], and the measurements are performed with an I–V monitor (Scientific Systems Inc, PIM) mounted on the powered electrode. The background pressure in the vacuum chamber is in the 10^{-7} Torr range and argon gas flows through the discharge chamber to maintain gas purity during the operation.

We use the EEDF measurement system to obtain the electron density and its axial profile. The EEDF measurements are performed using the r.f.-compensated Langmuir probe and AC superposition method [17]. A Langmuir probe made of tungsten wire 4 mm long and 0.15 mm in diameter is placed at the center of the two discharge electrodes. Fig. 2 shows the r.f.-compensated Langmuir probe system. The probe system is composed of a small probe tip and a floating-loop reference probe with choke coils that reduces r.f. distortion of the probe characteristics. The effect of the weak magnetic fields on the Langmuir probe is negligible because the probe radius is much smaller than the electron gyro radius [18]. Because there are many high-order harmonics in asymmetrically driven capacitive discharge [19], the r.f.-compensations for high-order harmonics are essential for EEDF measurements [20]. In this experiment, we used series-connected choke coils near the probe tip to reduce the higher harmonic distortions (1st, 2nd, 3rd) as shown in Fig. 2.

3. Experimental result and discussion

To obtain the r.f. sheath width at various magnetic fields, we use the I–V measurement method which obtains the effective sheath width ($2S_0 = \varepsilon_0 A/C_{sh}$), by means of calculating the discharge capacitance from the electrical measurements [13,16]. Generally total capacitance of the capacitive discharge could be expressed as following [14]

$$1/C_{tot} = 1/C_p + 1/C_g = S_p/\varepsilon_0 A_p + S_g/\varepsilon_0 A_g = \frac{\sqrt{\varepsilon_0/2en_e}}{\varepsilon_0}\frac{\sqrt{V_p}}{A_p}\left(1+\frac{\sqrt{V_g/V_p}}{A_g/A_p}\right) \quad (1)$$

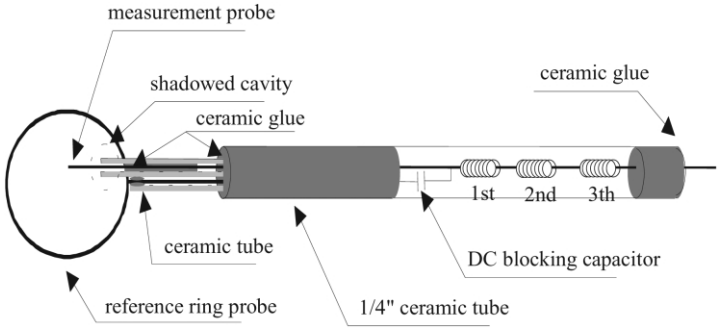

Fig. 2. R.f.-compensated Langmuir probe with series-connected choke coils.

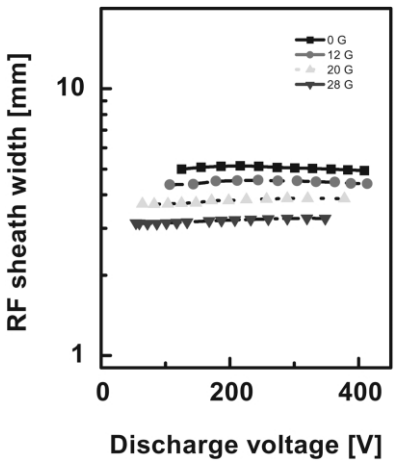

Fig. 3. R.f. sheath width at various magnetic fields.

where the sub-index 'p' and 'g' mean the powered electrode and grounded electrode. In our experiment, $A_p \sim A_g/2$ and $V_g/V_p \ll 1$ (V_p: 300–400 V, V_g: 20–25 V), so that we can neglect the second term in above equation.

$$1/C_{tot} \approx \frac{\sqrt{\varepsilon_0/2en_e}}{\varepsilon_0}\frac{\sqrt{V_p}}{A_p} = 1/C_p = S_p/\varepsilon_0 A_p \quad (2)$$

This means that total capacitance is approximately equal to that of the powered electrode sheath. As a result, we can obtain the sheath width of the powered electrode by means of capacitance measurement of the discharge.

Fig. 3 shows the sheath width characteristics at 10 mTorr with various magnetic fields (0–30 G). The experimental data at 0 G are consistent with those of Ref. [16] which investigated the electrical characteristics of the unmagnetized capacitive discharge. As in the previous reports [14,15], the r.f. sheath width decreases with increasing the magnetic field.

This could be understood by considering the sheath width characteristics of the transversely magnetized capacitive discharge. The sheath width of the transversely magnetized capacitive discharge can be expressed as [14]

$$S_0 \approx \sqrt{\frac{\varepsilon_0 V_m}{2en_e}} + \frac{L\omega^2}{4\omega_{pe}^2}\left(1 + \frac{\omega_c^2 + \nu^2}{\omega_{pe}^2}\right) \quad (3)$$

where V_m is an r.f. voltage, n_e is an electron density,ω_{pe} is a plasma frequency, ω is a driving frequency, L is gap distance and ν is an electron-neutral collision frequency. From the experimental condition $\omega_{pe} \gg \omega$, we can neglect the second term in Eq. (3).

$$S_0 \approx \sqrt{\frac{\varepsilon_0 V_m}{2en_e}} \quad (4)$$

The magnetic field effect on the sheath width is introduced in the above equation mainly through an electron density, because we use a fixed r.f. voltage [14]. The magnetic field could increase the electron density by reducing the electron diffusion toward the electrode [21]. Therefore, the sheath width would be decreased with increasing magnetic field as in the previous studies [14,15].

However, the magnetic field effect on the electron density is not simple as we mentioned above, i.e. a higher magnetic field does not always result in a higher electron density. According to Hutchison's report [22], the electron density decreases with increasing magnetic field until the magnetic field reaches 25 G, but after the magnetic field (25 G) the electron density increases with increasing magnetic field. It is due to the heating mode transition from collisionless to collisional heating by the magnetic field [11]. Therefore, the electron density decreases against the magnetic field in small magnetic field regime ($<$25 G), but the electron density increases against the magnetic field in large magnetic field regime ($>$25 G).

In our experiment, we also obtain a similar experimental result that of Ref. [22]. The EEPFs and the electron density measured by a Langmuir probe positioned at the discharge center are given in Fig. 4. The electron at the discharge center decreases with increasing magnetic field until 30 G, as shown in Fig. 4b. This decrease of electron density might result from not only a heating mode transition [11] but also a plasma bulk shift by a E×B drift expected effect in the magnetized capacitive coupled plasma (CCP) [23–25]. So there is no increase of electron density in this range of magnetic field (0–30 G). Therefore, the r.f. sheath width should increase with increasing magnetic field ($S_0 \propto 1/\sqrt{n_e}$). However, the sheath width decreases with increasing the magnetic field as shown in Fig. 3. It seems like a paradox.

We can solve this paradox by measuring the axial electron density profile of the discharge. Figs. 5 and 6 show the EEPFs and the axial electron density profiles with different magnetic fields at a fixed discharge voltage (300 V). The transverse magnetic field prevents electrons from moving to the axial direction by making a gyro-motion along the field line, so that ionization near the powered electrode is enhanced by electrons heated by an oscillating r.f. sheath field. As a result, increasing the magnetic field, while the electron density at the discharge center decreases by two effects mentioned above (E×B drift and heating mode transition),

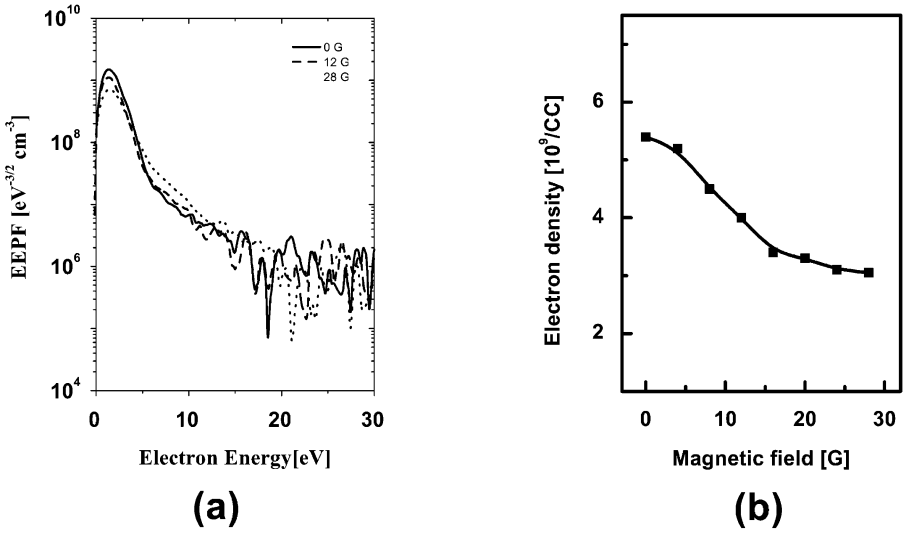

Fig. 4. EEPFs and electron density at the discharge center at 300 V with different magnetic fields.

the electron density near the powered electrode increases as shown in Fig. 6. Because the sheath width is influenced by the electron density near the sheath, the sheath width at the powered electrode decreases against the magnetic field.

4. Conclusion

We observed the paradoxical sheath width variation in the transversely magnetized capacitive discharge that the r.f. sheath width decreases with decreasing electron

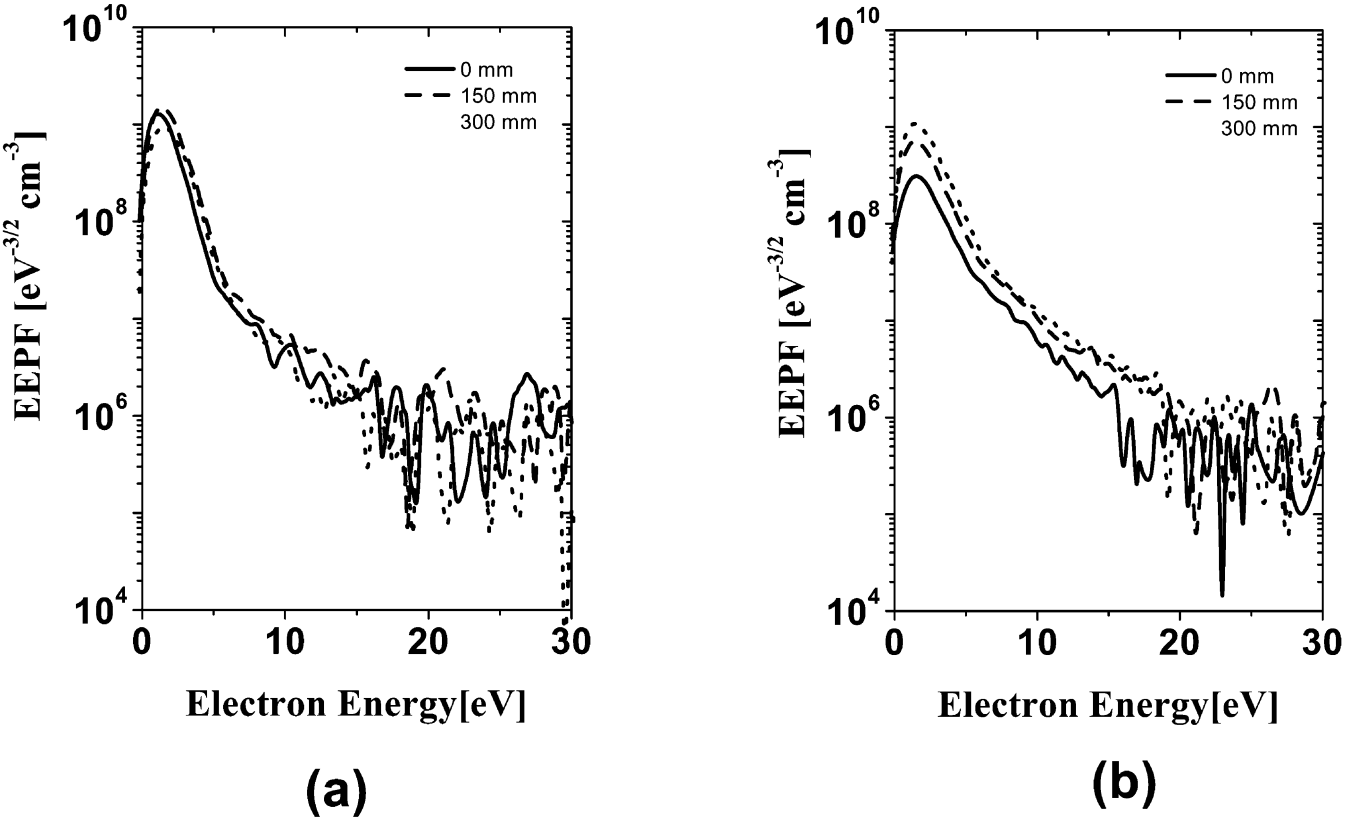

Fig. 5. EEPFs with axial distance from the grounded electrode at 300 V with different magnetic field (a) 0 G; (b) 28 G.

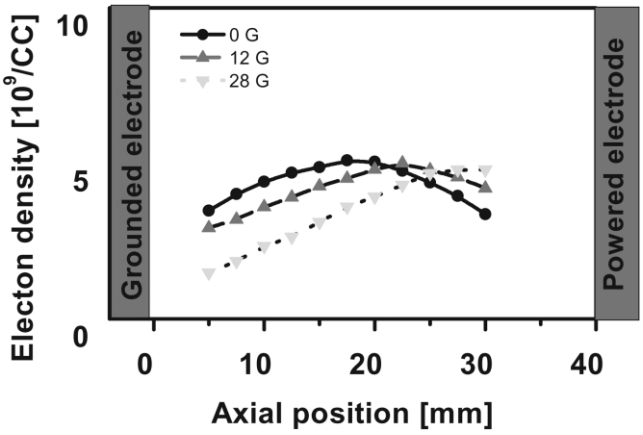

Fig. 6. Axial electron density profiles at 300 V with different magnetic fields.

density. This paradoxical result originates from the overlooking of the axial electron density profile variation by the magnetic field. Therefore, we can solve this paradox successfully by considering the axial electron density profile in the transversely magnetized capacitive discharge with Langmuir probe.

Acknowledgments

This work was sponsored in part by the SYSTEM I.C. 2010 of Ministry of Science and Technology (MOST) and Ministry of Commerce, Industry and Energy (MOCIE) and by grant from the Interdisciplinary Research Program of the KOSEF. This work was also supported in part by National Research Laboratory Project of Korea (M7-0104-00-0071). One of the authors thanks Plasmart Inc., for technical and financial support for this work.

References

[1] B. Chapman, Glow Discharge Process, Wiley, New York, 1980.
[2] M.A. Lieberman, A.J. Lichtenberg, Principles of Plasma Discharges and Materials Processings, Wiley, New York, 1994.
[3] J. Hopwood, C.R. Guarnier, S.J. Whitehair, J.J. Cuomo, J. Acad. Sci. Technol. A 11 (1993).
[4] V.A. Godyak, N. Sternberg, Phys. Rev. A 42 (1990) 4.
[5] M.A. Lieberman, IEEE Trans. Plasma Sci. 16 (1988) 638.
[6] M.A. Lieberman, IEEE Trans. Plasma Sci. 17 (1989) 338.
[7] V.A. Godyak, Soviet Radio Frequency Discharge Research Falls Church, Delphic, VA, 1986, p. 103.
[8] I. Langmuir, H. Mott-Smth, Phys. Rev. 23 (1924) 109.
[9] V.A. Godyak, N. Sternberg, IEEE Trans. Plasma Sci. 18 (1990) 159.
[10] C. Beneking, J. Appl. Phys. 68 (1990) 1.
[11] M.M. Turner, Phys. Rev. Lett. 75 (1995) 7.
[12] G. Gozakinos, M.M. Turner, D. Vender, Phys. Rev. Lett. 87 (2001) 13.
[13] V.A. Godyak, R.B. Piejak, N. Sternberg, IEEE Trans. Plasma Sci. 21 (1993) 4.
[14] J.C. Park, B. Kang, IEEE Trans. Plasma Sci. 25 (1997) 3.
[15] M.A. Lieberman, A.J. Lichtenberg, S.E. Savas, IEEE Trans. Plasma Sci. 19 (1991) 2.
[16] V.A. Godyak, R.B. Piejak, B.M. Alexadrovich, IEEE Trans. Plasma Sci. 19 (1991) 4.
[17] S.H. Seo, C.W. Chung, Phys. Rev. E 62 (2000) 5.
[18] R.R. Arslanbekov, N.A. Khromov, A.A. Kudryavtsev, Plasma Source Sci. Technol. 3 (1994) 4.
[19] V.A. Godyak, R.B. Piejak, B.M. Alexandrovich, Plasma Source Sci. Technol. 1 (1992) 1.
[20] T. Kubo, H. Kawata, Jpn. J. Appl. Phys. 36 (1997) 4601–4604.
[21] F.F. Chen, Introduction to Plasma Physics and Controlled Fusion, Plenum Press, 1983, p. 171.
[22] D.A.W. Hutchinson, M.M. Turner, R.A. Doyle, M.B. Hopkins, IEEE Trans. Plasma Sci. 23 (1995) 4.
[23] H. Shin, K. Noguchi, X.Y. Qian, N. Jha, G. Hills, C. Hu, IEEE Electron Dev. Lett. 14 (1993) 2.
[24] S. Nakagawa, T. Sasaki, H. Mori, T. Namura, Jpn. J. Appl. Phys. 33 (1994) 2194–2199.
[25] Y. Maemura, S.C. Yang, H. Fujiyama, Surf. Coat. Technol. 98 (1998) 1351–1358.